© 2022. Published by The Company of Biologists Ltd | Journal of Experimental Biology (2022) 225, jeb243119. doi:10.1242/jeb.243119

RESEARCH ARTICLE

Modular lung ventilation in *Boa constrictor*

John G. Capano[1,*], Scott M. Boback[2], Hannah I. Weller[1], Robert L. Cieri[3], Charles F. Zwemer[2] and Elizabeth L. Brainerd[1]

ABSTRACT

The evolution of constriction and of large prey ingestion within snakes are key innovations that may explain the remarkable diversity, distribution and ecological scope of this clade, relative to other elongate vertebrates. However, these behaviors may have simultaneously hindered lung ventilation such that early snakes may have had to circumvent these mechanical constraints before those behaviors could evolve. Here, we demonstrate that *Boa constrictor* can modulate which specific segments of ribs are used to ventilate the lung in response to physically hindered body wall motions. We show that the modular actuation of specific segments of ribs likely results from active recruitment or quiescence of derived accessory musculature. We hypothesize that constriction and large prey ingestion were unlikely to have evolved without modular lung ventilation because of their interference with lung ventilation, high metabolic demands and reliance on sustained lung convection. This study provides a new perspective on snake evolution and suggests that modular lung ventilation evolved during or prior to constriction and large prey ingestion, facilitating snakes' remarkable radiation relative to other elongate vertebrates.

KEY WORDS: XROMM, Biomechanics, Constriction, Ingestion, Snake, Ventilation

INTRODUCTION

There is a surprising discrepancy in species richness, distribution and ecological scope among elongate vertebrates. The clade Serpentes is a spectacular outlier, with more than 3700 known species that occupy every continent except Antarctica and are found in extremely diverse habitats including terrestrial, fossorial, arboreal, freshwater and marine (Capano, 2020; Hsiang et al., 2015; Uetz et al., 2019). In contrast, snakes' closest rivals among elongate vertebrate clades, Anguilliformes (919 spp.), Gymnophiona (213 spp.) and Amphisbaenia (201 spp.), have similar divergence times yet have far fewer species, are geographically limited and are constrained to primarily aquatic and fossorial environments (Bergmann et al., 2020; Uetz et al., 2019). In addition, the evolution of an elongate body form is a common theme within vertebrates, having independently evolved at least 65 times within Vertebrata, including 25 times within Squamata alone (Bergmann et al., 2020; Brandley et al., 2008). Given that the evolution of elongation is more commonplace than extraordinary, what trait or traits within snakes have set them apart and enabled this extensive radiation relative to other elongate vertebrates?

The evolutionary mechanisms behind the rampant diversification of snakes are not entirely clear (Brandley et al., 2008; Caldwell, 2019; Gans, 1961; Greene, 1983; Greene and Burghardt, 1978; Wiens et al., 2006). Several innovations have been proposed as explanations of their success, but two key evolutionary events in particular stand out: (1) constriction behavior and (2) highly kinetic skulls (Caldwell, 2019; Greene, 1983; Greene and Burghardt, 1978; Longrich et al., 2012). Both of these features contributed to the emergence of macrostomy, the capacity to consume whole prey with large cross-sectional area, in snakes, by allowing snakes to either subdue (constriction) or ingest (highly kinetic skulls) prey exceeding 100% of their body mass (Greene, 1997). This remarkable ability to subdue and consume such massive prey may have facilitated entry into novel ecological niches, yet these behaviors are not without mechanical and physiological obstacles that early snakes must have overcome. Constriction, ingestion and digestion of large prey all have the potential to spatiotemporally inhibit lung inflation. These behaviors may have severely limited the rib and body wall movements necessary for ventilation as a result of body wall compression during constriction and visceral cavity displacement during ingestion and digestion (Secor, 2008). Thus, snakes may have needed to circumvent the constraints on lung ventilation before constriction and macrostomy could evolve.

For snakes, a mechanical constraint on ventilatory motions would be particularly detrimental because they have no accessory ventilation mechanism (e.g. the diaphragm of mammals) and thus rely entirely on motions of their ribs (Brainerd, 2015; Brainerd and Owerkowicz, 2006). A possible solution would be to shift the location of ventilatory rib motions away from the constrained regions and instead use an unencumbered region of their elongate bodies. Such a behavior has been anecdotally described in multiple observations, where snakes appeared to shift the location of ventilation within their trunk in response to coil application during constriction or body wall distention during ingestion (e.g. Movie 1) (Canjani et al., 2003; Greene, 1997; Lillywhite, 2014; McDonald, 1959; Rosenberg, 1973; Wallach, 1998). However, this plausible behavior has never been empirically studied and it is unclear whether the apparent spatial shift of ventilatory movements involves active actuation of rib movements in some body regions and quiescence in others. An alternative possibility could be that the entire rib cage attempts lung ventilation, but motions are only observed in unconstrained regions, such as those not around either the constriction coil or ingested prey bolus.

However, we propose that the potential for snakes to actively shift the location of lung ventilation throughout their trunk is plausible based on the previous qualitative observations and the anatomy of snakes. Snakes use their ribs to breathe, and these motions are driven primarily by a robust, serially repeated hypaxial muscle, the levator costa (LC) (Fig. 1), not typically found in other squamates (Carrier,

[1]Department of Ecology and Evolutionary Biology, Brown University, Providence, RI 02912, USA. [2]Department of Biology, Dickinson College, Carlisle, PA 17013, USA. [3]School of Science and Engineering, University of the Sunshine Coast, Maroochydore, QLD 4558, Australia.

*Author for correspondence: (john_capano@brown.edu)

J.G.C., 0000-0001-7558-3704; R.L.C., 0000-0001-6905-9148; E.L.B., 0000-0003-0375-8231

Received 2 July 2021; Accepted 11 February 2022

Journal of Experimental Biology (2022) 225, jeb243119. doi:10.1242/jeb.243119

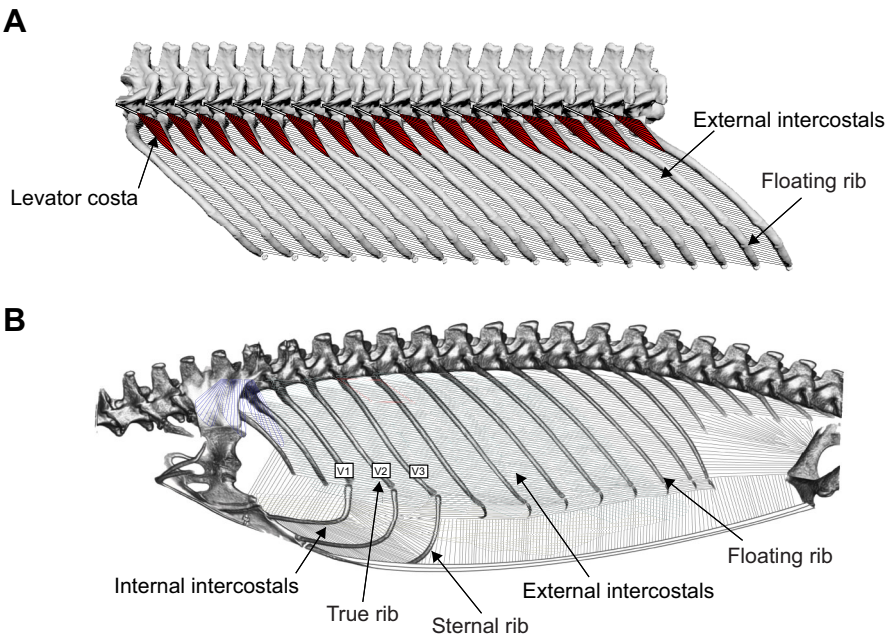

Fig. 1. Axial anatomy of snakes and representative non-snake squamates. Cranial is to the left in both images. (A) Generalized precloacal axial skeleton of *Boa constrictor*. Levator costae (red) are hypaxial muscles that run from the prezygopophysial process of each vertebra to the cranial side of the proximal third of each rib. External intercostals (black lines) are the only intercostals present in snakes (Gasc, 1981; Penning, 2018; Rosenberg, 1973). Floating ribs lack ventral connections. (B) Axial skeleton of *Varanus exanthematicus*, a non-snake squamate with floating ribs that contribute to lung ventilation (Cieri et al., 2018). External (dorsoventral black lines) and internal intercostals (ventrodorsal black lines) are typically synchronously active during lung ventilation in most non-snake squamates (Carrier, 1989). True ribs consist of a dorsal rib connected to a sternal rib via an intracostal joint. Floating ribs have no ventral connections, as in snakes, and are morphologically reminiscent of those of snakes. V1–3; vertebral ribs 1–3.

1989; Rosenberg, 1973; Young and Kardong, 2010). The LC is present on all 200+ pairs of ribs in snakes (Fig. 1A), which are found on almost every vertebra, from neck to cloaca. Snake ribs are distinct from 'true' ribs used during ventilation by most amniotes and are morphologically analogous, if not homologous, to 'floating' ribs present in other amniote taxa (Fig. 1) (Cohn and Tickle, 1999; Gasc, 1981; Head and Polly, 2015; Hoffstetter and Gasc, 1969). Within this extensive framework of ribs is a highly elongate and asymmetrical lung, with the right lung of more basal constrictors, such as boas and pythons, extending one-third of their snout–vent length (SVL), while the left is highly reduced (Hsiang et al., 2015; Kardong, 1972; Wallach, 1998). The lungs of snakes are also heterogeneous and have a discrete 'vascular' region in the cranial portion that abruptly transitions to an avascular 'saccular' region with insufficient blood flow for effective gas exchange (Grant et al., 1981; Wallach, 1998). Numerous hypotheses have been proposed for the function of this saccular region, including acting like a caudal bellows to draw air through the vascular region when lung ventilation mechanics are hindered in more cranial segments, such as during constriction and prey ingestion (Gratz et al., 1981; McDonald, 1959; Wallach, 1998).

To determine whether and how snakes may relocate ventilation during constriction and large prey ingestion requires data on airflow, muscle activation and *in vivo* rib kinematics, which are difficult to obtain. The innovation of XROMM (X-ray reconstruction of moving morphology) in recent years has made it possible to reliably quantify such *in vivo* bone motion and empirically address this phenomenon in snakes. In the current study, we used a combination of XROMM, pneumotachography, electromyography and videography to test our hypothesis that snakes actively modulate the location of lung ventilation throughout their trunk in response to hindered rib motions. We used the boa constrictor, *Boa constrictor* Linneaus 1758, as our study species because of its consistent constriction coil application, ability to consume extreme prey sizes, and more basal divergence within Macrostomata (Hsiang et al., 2015; Mehta and Burghardt, 2008). We used XROMM to quantify rib rotations throughout the trunk of boa constrictors during lung ventilation (i) at rest and (ii) while restricting rib motions in either the vascular or saccular regions, through controlled application of a blood pressure cuff. We used pneumotachography and the corresponding X-ray videos during some trials to associate airflow with rib motion. Electromyography was used to quantify whether LC muscles throughout the trunk were synchronously activated or could independently produce rib motion in either the vascular or saccular region. We also used videography to document *in vivo* lung ventilation patterns during constriction, prey ingestion and other relevant behaviors in our study. We then compared our XROMM rib motion data from boas with the ventilatory kinematics of three previously studied non-serpentine squamates to gain insight into potential mechanisms and functional differences that would produce or preclude modular lung ventilation in snakes (Brainerd et al., 2016; Capano et al., 2019a; Cieri et al., 2018). Lastly, we layered these quantitative and qualitative data to holistically answer whether boa constrictors can actively modulate the location of lung ventilation throughout their trunk and discuss the potential role of modular lung ventilation in the evolutionary success of Serpentes.

MATERIALS AND METHODS

We conducted part of this study at Brown University and part at Dickinson College. For the XROMM portion of this study conducted at Brown University, we used three adult female boa constrictors that varied from large to moderately sized (boa01, 11.6 kg; boa02, 3.4 kg; boa03, 6.1 kg). We used five separate boa constrictors for the electromyography and videography portion of this study conducted at Dickinson College. For electromyography, we used an adult female and male (boa04, 1.64 kg; boa05, 0.83 kg) and for videography we used two adult males and one adult female (boa06, 1.8 kg; boa07, 1.4 kg; boa08, 2.24 kg). One individual used for the Brown University portion was acquired from a reputable reptile breeder. The remainder of the animals were captive-born (F1 and F2 generation) snakes bred from individuals wild-caught in Belize, Central America. Snakes were maintained in a climate-controlled animal care facility (28±2°C, 60% relative humidity) on a diet of dead rats. All animal husbandry and experimental procedures for each respective portion were approved by the Institutional Animal Care and Use Committee of Brown University or Dickinson College.

Journal of Experimental Biology (2022) 225, jeb243119. doi:10.1242/jeb.243119

XROMM data collection

To quantify individual rib motions, we produced 3D bone animations of *in vivo* behavior with marker-based XROMM (Brainerd et al., 2010). We implanted a minimum of three radio-opaque markers into each vertebra and rib of interest, with effort to maximize inter-marker distances and avoid collinearity to increase rigid-body accuracy (Brainerd et al., 2010). All individuals had ribs marked in the middle of the vascular lung region (approximately 35% SVL) and in the middle of the saccular lung region (approximately 50% SVL) (see Supplemental Materials and Methods for technical details and Table S2 for individual marker sets). These locations were determined through visual observations, preliminary computed tomography (CT) scans and published anatomical descriptions for the species (Wallach, 1998).

We collected X-ray video data from vertebrae and ribs over the vascular and saccular lung regions to compare rib motion patterns throughout the trunk. We prioritized obtaining the largest possible breaths, including those during defensive hissing, to capture maximal rib excursion and facilitate comparison with previous data on deep breathing in non-snake squamates (Brainerd et al., 2016; Capano et al., 2019a; Cieri et al., 2018). We quantitatively and qualitatively determined that hissing produced among the largest magnitude changes from maximal exhalation to maximal inhalation (Table 1) (Duncker, 1978; Gans and Maderson, 1973; Grant et al., 1981; Lillywhite, 2014). Hissing was also the only behavior that did not require experimental manipulation (see below) to elicit rib motions within the saccular region. We therefore did not differentiate large breaths from hissing because these constituted some of the largest measurable breaths and aligned with our objective of measuring maximal rib excursion during ventilation throughout the trunk.

With the aim of quantifying whether boas could modulate the location of lung ventilation in response to hindered rib motions, we produced consistent and controlled rib motion obstruction through application of a blood pressure cuff (Model BPAG1-20CVS; CVS, Woonsocket, RI, USA). We wrapped the cuff around the marked ribs in the vascular or saccular regions and incrementally applied compressive pressure until rib motions ceased in that region (approximately 180–210 mmHg). When the vascular region was obstructed, we recorded motions in the saccular region and vice versa, although cuff application was unnecessary to elicit motion in the vascular region. In a few trials, we were able to simultaneously record both regions when the animal was fortuitously positioned in the X-ray field.

We collected CT scans to produce 3D coordinates and polygon meshes of our markers and bones. All scans were collected with a Fidex Animage veterinary scanner at Brown University (Fidex, Animage, Pleasanton, CA, USA; 110 kV, variable mA, 0.173 mm slice thickness). We created our 3D polygonal mesh surface models of vertebrae, ribs and the corresponding radio-opaque markers with the open-source medical imaging software Horos (Purview, Annapolis, MD, USA). The raw data used in this study (X-ray video data and CT scan data) are available on the X-ray Motion Analysis Portal (www.xmaportal.org) under the public collections associated with permanent ID Brown63 and are stored in accordance with best practices for video management in organismal biology (Brainerd et al., 2016). We analyzed all biplanar X-ray videos with XMALab (www.xromm.org) to track the 3D coordinates of each marker and generate rigid-body transformations for bone animations (Knörlein et al., 2016). Our marker tracking precision

Table 1. Rotation magnitudes calculated from maximal exhalation to maximal inhalation for a single rib from each breath analyzed in *Boa constrictor*

					Rotation (deg)		
Individual	Location	Behavior	Rib	Breath	Pump (*X*)	Caliper (*Y*)	Bucket (*Z*)
boa01	Vascular	Rest	rib01L	1	−19.9	12.9	29.9
	Vascular	Rest	rib01L	2	−11.7	10.2	23.8
	Vascular	Rest	rib01L	3	−16.4	3	20.7
	Vascular	Rest	rib01L	4	−17.7	7.2	24.4
	Vascular	Rest	rib01L	5	−17	10.8	28.9
	Vascular	Rest	rib01L	6	−24.5	13.4	31.7
	Saccular	Rest	rib02L	7	−5.5	1.2	13.1
	Saccular	Rest	rib02L	8	−3.5	1.8	8.1
	Saccular	Rest	rib02L	9	−2.9	0.5	5.9
	Saccular	Rest	rib02L	10	−0.8	2.6	10.8
boa02	Vascular	Hiss	rib02L	1	−26.2	4.4	33.3
	Vascular	Hiss	rib02L	2	−24	5.4	37
	Vascular	Hiss	rib02L	3	−27.4	3.2	30.1
	Vascular	Hiss	rib02L	4	−22.7	4.2	33.2
	Vascular	Hiss	rib02L	5	−22.9	5.5	44.6
	Vascular	Rest	rib02L	6	−11.1	8.9	18.9
	Saccular	Rest	rib02R	7	−2.8	2.6	9.5
	Saccular	Rest	rib02R	8	−2.3	2.7	12.2
	Saccular	Rest	rib01L	9	−4.2	1.5	22.7
	Saccular	Rest	rib01L	10	−5.6	1.8	24.2
	Saccular	Rest	rib01L	11	−5	2.9	24.3
boa03	Vascular	Hiss	rib03L	1	−17	3.3	35.3
	Vascular	Hiss	rib03L	2	−13.8	1.1	35.1
	Vascular	Rest	rib03L	3	−14.1	10	39.8
	Vascular	Rest	rib04L	4	−6.7	8	14.7
	Vascular	Rest	rib04L	5	−6.7	10	19.2
	Saccular	Hiss	rib04L	6	−24.3	13	44.1
	Saccular	Rest	rib04L	7	−7.1	12.3	35.3
	Saccular	Rest	rib04R	8	−4.7	1.7	20

was 0.0055 mm (best pairwise s.d. was 0.0024 mm; worst was 0.0244 mm), indicating that our marker sets did not move appreciably within each rigid body. In a handful of instances, we used 'virtual' markers to increase animation accuracy similar to scientific rotoscoping (see Supplemental Materials and Methods) (Gatesy et al., 2010).

The tracked 3D coordinates of each marker were then used to calculate rigid-body transformations to drive our bone animations. Transformations were filtered with a Butterworth low-pass filter within XMALab (cut-off frequency 0.5–5 Hz) to smooth non-biological noise (Knörlein et al., 2016). Each transformation was then applied to the corresponding bone model within Autodesk Maya. We animated and analyzed the largest breaths in the vascular and saccular lung regions during lung ventilation at rest, with the blood pressure cuff applied to each region, and during hissing bouts. A breath cycle was defined as maximal exhalation to maximal inhalation and the ribs chosen to animate depended upon visibility within the X-ray videos. Ten breathing cycles were animated for boa01, 11 for boa02 and nine for boa03, with variation in the number and sidedness of ribs between trials and individuals (see Table S1).

Pneumotachography

In some XROMM trials, we used pneumotachography to measure airflow. This was inconsistent among trials because snakes often removed the pneumotach apparatus during a trial. Our pneumotach data were therefore not consistently calibrated for volume per minute but were sufficient to record pressure variation and estimates of volume change associated with exhalation and inhalation, which we visually confirmed in X-ray videos when possible. Following techniques used in similar lung ventilation studies, we fabricated a small lightweight mask from a 500 ml plastic bottle, with a PVC extension from the cap hole that was divided with an 88 µm screen (Landberg et al., 2003). A differential pressure transducer (Validyne DP103-06; Northridge, CA, USA) was connected to ports on either side of the mesh and used in series with a pneumotachograph to measure airflow (Fig. S1). All pneumotachography data were recorded with PowerLab data acquisition hardware and LabChart software (ADInstruments, Colorado Springs, CO, USA), calibrated following procedures in similar experiments, and synchronized with the X-ray trigger system (Landberg et al., 2003).

Electromyography

We used electromyography in two boas to quantify whether LC were capable of spatially discrete patterns of activation. A patch electrode was implanted on the LC over the middle of the vascular portion of the lung (approximately 35% SVL) and over the middle of the saccular portion of the lung (approximately 50% SVL) in each animal (see Supplemental Materials and Methods for electrode fabrication and technical details). These locations were determined through visual observations and anatomical descriptions for the species, and subsequently confirmed via dissection (Wallach, 1998). A handful of trials were simultaneously recorded with light video cameras (GoPro, Half Moon Bay, CA, USA) at 25 frames s^{-1} and intermittently synced through inclusion of EMG signal time stamps into the video recordings. All data were collected within 7 days of electrode implantation and EMG signals were postprocessed with R package 'biosignalEMG' using 100 and 300 Hz lowpass and highpass filters, respectively (Guerrero and Macías-Díaz, 2014). In the one fortuitous EMG trial for which GoPro video data were also collected, we synced the time stamps of our EMG and video recordings to associate muscle activity with externally observable lung ventilation motions.

Analyses

We measured all skeletal kinematics with joint coordinate systems (JCSs) to capture the complex 3D rotations of each rib (Grood and Suntay, 1983). Rib rotations were measured relative to three anatomical axes (Fig. 2A) with non-naturally occurring reference poses to facilitate interspecies comparisons (see Supplemental Materials and Methods). The rotations of each rib are best described with terminology that has become convention in many contemporary ventilation studies (Brainerd, 2015; Brainerd et al., 2016; Brocklehurst et al., 2017; 2019; Capano et al., 2019a; Cieri et al., 2018; De Troyer et al., 2005). These rotations consist of 'bucket handle' rotation about a dorsoventral axis (Fig. 2B), 'caliper' rotation about a craniocaudal axis (Fig. 2C) and 'pump handle' rotation about a mediolateral axis (Fig. 2D). Each axis is modeled as a pin joint about which each rotation occurs, i.e. bucket handle rotates cranial and caudal about a dorsoventral hinge, caliper rotates dorsal and ventral about a craniocaudal hinge, and pump handle is long-axis rotation or 'twisting' about the neck of the rib.

For our analyses, we needed to both (i) compare rib rotations between hindered and unhindered regions and (ii) determine whether all measured rotations could be binned as descriptive for boa constrictors as a species. All analyses were performed in R software (version 4.0.2) and we considered tests significant at the level of $P \leq 0.05$ (http://www.R-project.org/). We only collected four manipulation trials with the blood pressure cuff applied where the vascular and saccular regions could be measured simultaneously (see Table 1). We compared the raw rotational magnitudes of each axis between these regions with a two-way ANOVA while accounting for individual variation and calculated *P*-values with the R package 'lme4' (Bates et al., 2015).

Our XROMM dataset quantifying the rib kinematics of boas as a species included multiple sources of biological variation, with breaths recorded in different postures, behaviors and locations on the body (Figs S2–S4). We therefore used mixed effects models to test how these variables affected our measurements (and whether they could be descriptive for the species) and used the same packages for fixed and random effects for consistency (see Table S1). We used the R package 'lme4' to construct multiple linear mixed-effects models for each rotational axis of each individual, accounting for the following random effects: rib number, posture, behavior and rib location, as well as their interactions (Bates et al., 2015). Models were compared with a two-way ANOVA and *P*-values were calculated with R package 'lmerTest' using a Type III ANOVA with Satterthwaite's method (Kuznetsova et al., 2017).

The nature of our dataset and differences in snake behavior produced variation in our rib rotation magnitudes that we needed to account for prior to interspecific comparisons. We found no significant effect of posture in any individual, while behavior was significant only for bucket and pump handle rotations in boa02 (P_Z=0.002; P_X<0.000) and caliper rotations in boa03 (P_Y=0.045). Rib location was significant only for bucket and pump handle rotations in boa01 (P_Z<0.01; P_X<0.01) and pump handle rotations in boa02 (P_X=0.02). While saccular rib rotations during hissing were consistent, we could only elicit isolated rib rotations over the saccular region when the blood pressure cuff was applied. Trial-specific variation in animal behavior resulted in some manipulation trials eliciting breaths on top of our marker set while others were more cranial or caudal to the marked ribs. This produced magnitude differences that were not biologically relevant, because all ribs were capable of the same range of rotational magnitudes, and variation

Journal of Experimental Biology (2022) 225, jeb243119. doi:10.1242/jeb.243119

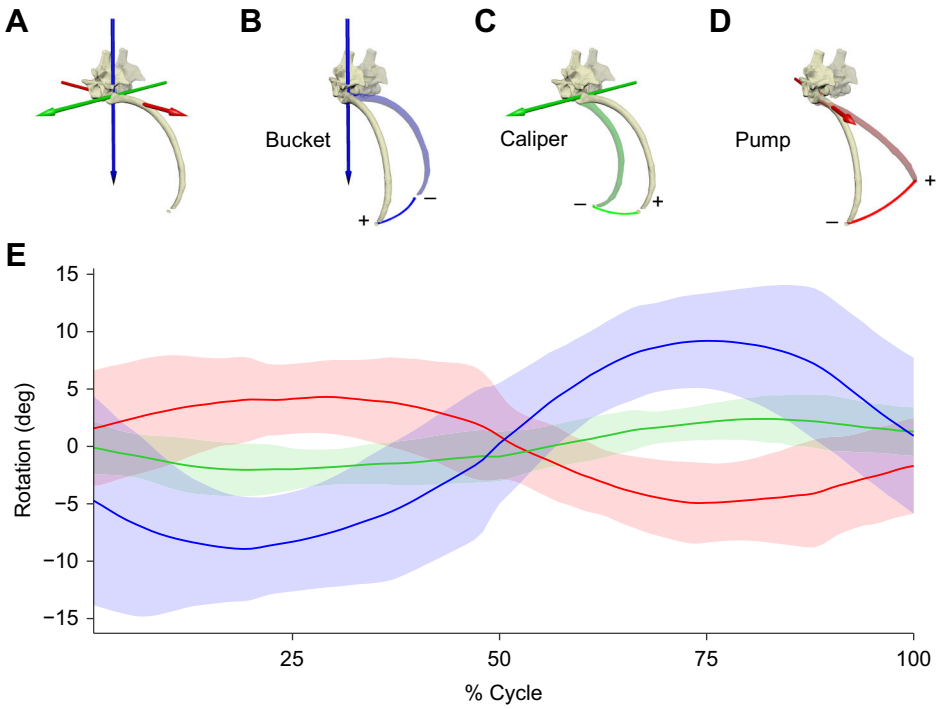

Fig. 2. Three-dimensional rib rotation axes and mean rib rotations during lung ventilation in *B. constrictor*. Cranial is to the left in all images. (A) The three axes that describe rib rotations are oriented relative to anatomical axes (45 deg oblique view) with bucket, caliper and pump rotation terminology following (Osmond, 1985). Costal rotations are measured about each costovertebral joint as interdependent Euler angles with *ZYX* rotation order and polarity set with the right-hand rule. The colored arrow or axis of rotation is best described as a pin joint about which each rotation occurs. (B) Bucket handle motion is cranial–caudal rotation about a dorsoventral axis (blue arrow;+is cranial rotation). (C) Caliper motion is dorsal–ventral rotation about a craniocaudal axis (green arrow;+is dorsal rotation; 45 deg oblique view). (D) Pump handle motion is long-axis rotation about a mediolateral axis (red arrow;+is caudal rotation; 70 deg oblique view). Long-axis rotation about the neck of the rib rotates the rib tip cranial–caudal and dorsal–ventral. (Note: colored parts are the distal rib tip trajectory during rotation about each axis; transparent colored ribs are rib positions after rotation). (E) Mean rib rotation angles during lung ventilation in *B. constrictor* with angles zeroed and time normalized to 100% breath duration. Each breath was defined as exhalation followed by inhalation (maximum exhalation is at 25% cycle; maximum inhalation is at 75% cycle). Solid line shows mean cycle (n=56 individual rib rotations) and shading shows ±s.d.

was produced as a result of the large magnitudes used during hissing and variability in the specific ribs used within each trial.

We therefore had to account for this variation due to behavior and rib location to understand boa-specific kinematic pathways. We calculated the residuals of a multivariate linear model fitting raw rotational magnitudes as a function of behavior and rib location. These residuals represented variation in rib rotations between individuals while accounting for the effect of behavior and rib location. We then centered the residuals on the mean rotational centroid matrix (see below) to categorize rib rotations of boas as descriptive for the species (see Table S1). Our residual-corrected rib rotation magnitudes had no influence on average rotations (Table S1) and reduced the s.e.m. of bucket handle, caliper and pump handle rotations to ±0.9, ±0.6 and ±0.6 deg, respectively.

We subsequently coalesced the raw rib rotation magnitudes from datasets of three previously studied non-snake squamates to compare with our boa data. For these three lizard species, we only used rotations that were not statistically different from other ribs within each species. We used rotations from the first vertebral rib of the green iguana, *Iguana iguana* (Linneaus 1758), all ribs of the savannah monitor lizard, *Varanus exanthematicus* (Bosc 1792), and the first vertebral rib of the Argentine black and white tegu, *Salvator merianae* Duméril and Bibron 1839 (Brainerd et al., 2016; Capano et al., 2019b; Cieri et al., 2018). We then used each species' rotational magnitudes to calculate species-specific *XYZ* matrix centroids. The rotational magnitudes were then divided by their root means square and the centroid subtracted from this value to normalize the data with respect to magnitude. We constructed multiple multivariate linear mixed effect models for all species' rotations while accounting for the fixed effects of axis×species and rib type and the random effect of individual, with R package 'lme4' (Bates et al., 2015). Models were compared with either a one- or two-way ANOVA and *P*-values were calculated with R package 'lmerTest' using a Type III ANOVA with Satterthwaite's method (Kuznetsova et al., 2017).

RESULTS

Rib kinematics and modular lung ventilation in boa constrictors

We found multiple lines of evidence in support of our hypothesis that boa constrictors actively modulate the trunk segments and ribs used for lung ventilation, in response to hindered rib motions. We found that individuals ventilated with the saccular region only when (i) the vascular region was restricted with the blood pressure cuff or (ii) the snake inflated the entire lung (vascular and saccular) during hissing. In the 11 analyzed saccular breaths elicited with blood pressure cuff application, we found substantial rib rotations in the saccular region (Table 1; Table S1) and visually confirmed no rib rotation in, or adjacent to, the restricted portion of the vascular lung region. As a control, we also collected X-ray videos in which the blood pressure cuff was applied to the vascular region with no pressure applied. In these instances, we found that individuals continued to use rib motions in the vascular region. During constriction, we found that the boas ventilated in trunk segments

Journal of Experimental Biology (2022) 225, jeb243119. doi:10.1242/jeb.243119

caudal to their constriction coil (Movie 1). We likewise confirmed that during prey ingestion, boa constrictors performed lung ventilation with segments around the prey bolus and appeared to shift as the bolus progressed further into the body (Movie 1). Moreover, we qualitatively documented one individual breath with two separate body segments, with no motion apparent in the segment between them (boa09).

These observations were further validated by four fortuitous breaths where both the marked vascular and saccular regions were simultaneously visible in the X-ray videos. In one trial (Table 1; boa03, breaths 4 and 5), the blood pressure cuff was applied to the saccular region, and we measured substantial rib rotations in the vascular region, no rib or cyclical motion in the saccular region, and pneumotach confirmation of airflow (Fig. 3; Movie 2). In two separate trials where the blood pressure cuff was applied to the vascular region (Table 1; boa02, breaths 9–11; boa03, breath 8), we measured no rib or cyclical motion in the vascular region, substantial rib rotations in the saccular region, and pneumotach confirmation of airflow (Fig. 3; Movie 3). The one exception was a single trial with the blood pressure cuff applied to the vascular region (Table 1; boa02, breaths 7 and 8), and rib motions occurred throughout the trunk. This trial does not preclude the capacity for

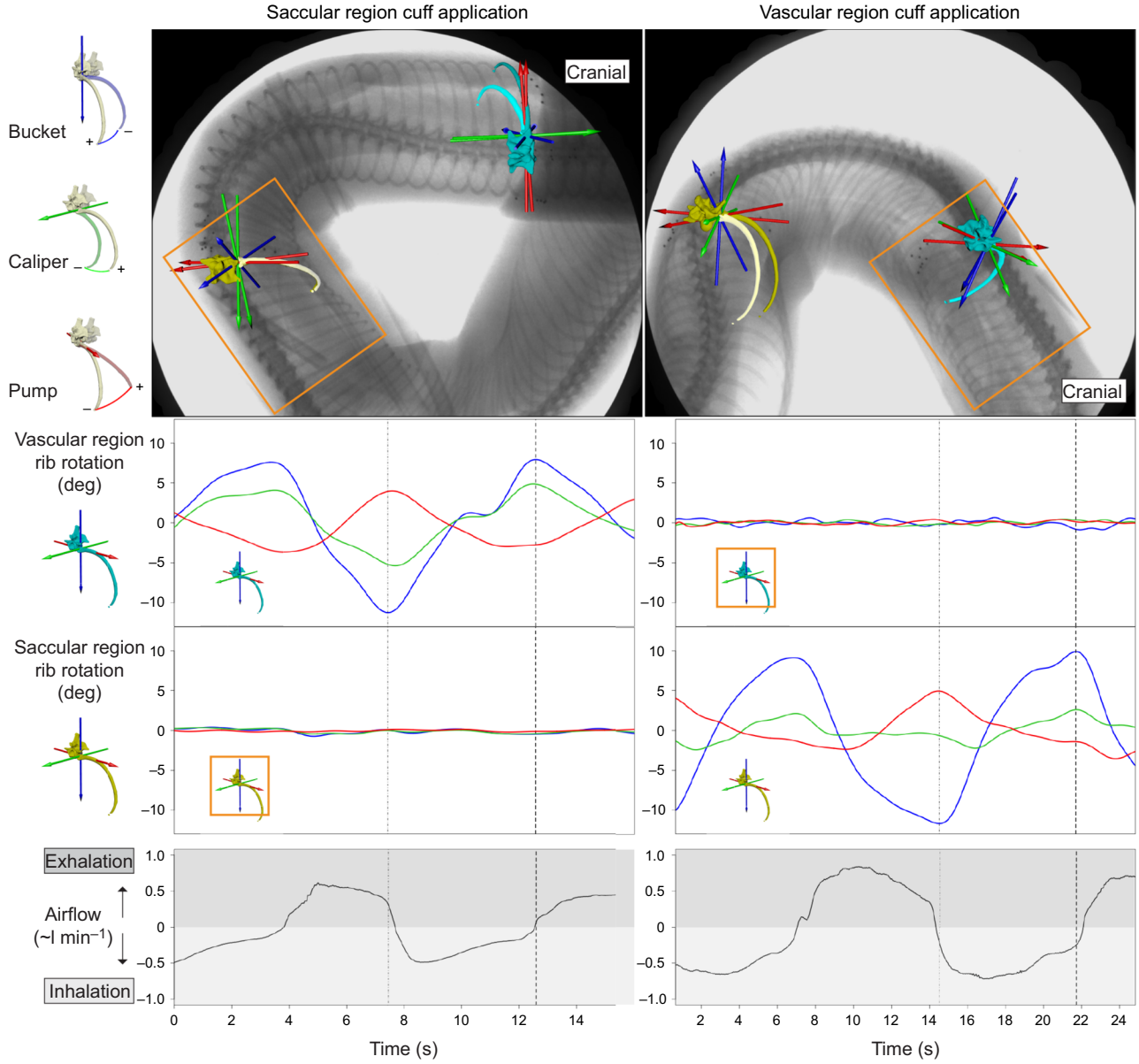

Fig. 3. Modular rib rotation mechanics during lung ventilation in *B. constrictor* produced with blood pressure cuff application. Rib rotation and airflow measurement in experiments with rib rotations hindered in cranial or caudal regions via blood pressure cuff application. Body region and ribs where the cuff was applied are marked with an orange rectangle. All traces show inhale–exhale–inhale. The light dashed line indicates maximal exhalation; the heavy dashed line indicates maximal inhalation; luminous colored ribs show rib position at maximal exhalation. Left: cuff application around the saccular region, in the more caudal portion of the lung, produced substantial rib rotation in the vascular region, no rib or cyclical motion in the saccular region, and ventilatory airflow. Right: cuff application around the vascular region, in the more cranial portion of the lung, produced an active shift of the location of ventilation and we measured no rib or cyclical motion in the vascular region, substantial rib rotation in the saccular region, and ventilatory airflow. Note: incandescent ribs overlap non-incandescent models in regions where the cuff is applied. We did not observe rib motions at the edges of the cuff that would suggest attempted rib rotations throughout the entire trunk (see Movies 2 and 3).

Journal of Experimental Biology (2022) 225, jeb243119. doi:10.1242/jeb.243119

discrete motions but, like hissing, demonstrates snakes' ability to use rib motions throughout the full lung length. Moreover, we found that the minor rotations of the hindered ribs were significantly smaller than unhindered ones and likely a result of marker centroid digitization, where inconsistent tracking of marker centroids results in rotational noise (Brainerd et al., 2010). The fluctuations we measured also had no cyclical or biologically relevant pattern and were often within the precision limits of JCS measurements of other studies (Brainerd et al., 2016; Brocklehurst et al., 2019; Menegaz et al., 2015).

We found that our hindered rib kinematics contrasted with all other rib rotations measured in boas. All non-hindered rib rotations followed a general kinematic pattern, with the raw and centroid normalized rotational magnitude being predominantly bucket handle rotation (mean±s.e.m.: raw 24.7±1.3 deg, normalized 0.73±0.026 deg), with small amounts of caliper rotation (mean±s.e.m.: raw 5.4±0.6 deg, normalized 0.16±0.014 deg), and substantial amounts of pump handle rotation (mean±s.e.m.: raw −13.6±0.6 deg, normalized −0.4±0.019 deg) (Table 1, Figs 2 and 4). When we compared our hindered rib motions with the raw unhindered rotations, we found that they were significantly different for all three rotational axes (P_Z<0.001; P_Y<0.001; P_X<0.001).

Using EMG, we further found that boas could activate LC muscles in spatially discrete body regions at will. Throughout bouts of prolonged hissing in boa04, we recorded simultaneous activity of the LC in the vascular and saccular regions, associated with full body inflation and deflation (Fig. S5). In recordings of lung ventilation at rest in boa05, we documented activity of the LC in the vascular region while activity in the saccular region was quiescent (Fig. S6). In a subsequent trial, the snake coiled the cranial portion of its body in preparation to strike and we recorded activity of the LC in the caudal saccular region while the vascular region was inactive (Fig. S6).

Comparison with non-snake squamates

When we compared rib rotations among our four species with our multivariate linear mixed effect models, we found consistent patterns in boas and monitor lizards that differed from those in iguanas and tegus (Fig. 4). When comparing the specific effects of axis×species while controlling for the random effect of individual, our omnibus ANOVA found that species was a significant predictor of rib rotations ($F_{3,11.89}$=6.27; P=0.009). Specifically, our mixed effects model found that the rib rotations of iguanas and tegus were significantly different from those of boas (P<0.001; P<0.001), while those of monitor lizards were not (P=0.99). An important distinction we found was that, unlike iguanas and tegus, the pump handle rotations of both boas and monitors was negative (Fig. 4A), indicating that during inhalation the latter two species used cranial pump handle rotations while the former two used caudal pump handle rotations.

When we additionally included the fixed effect of rib type (i.e. differences between vertebral and floating ribs), the corresponding analyses found the same levels of significance for species overall ($F_{3,13.15}$=8.92; P=0.002) and for each species relative to boas (iguanas: P<0.001; monitors: P=0.44; tegus: P<0.001). We also found, however, that rib type was a significant predictor of rib

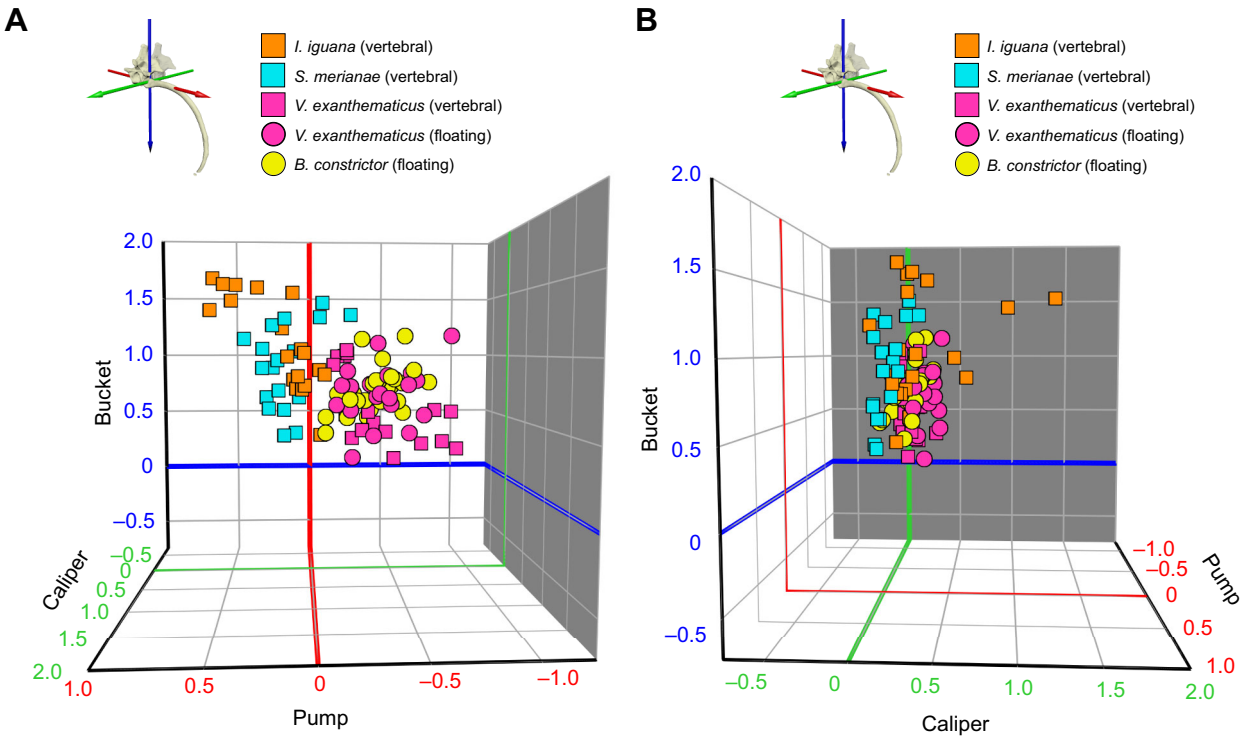

Fig. 4. Centroid-normalized 3D scatter plot of rib rotation magnitudes in four species of squamates. All analyzed breaths for each species were normalized relative to their 3D matrix centroid to assess interspecific kinematic patterns. Each point corresponds to the kinematic pathway of a discrete rib rotation as a function of the relative contribution from each rotational axis while including polarity from maximal exhalation to maximal inhalation. (A) Orthogonal view of the relative proportion of bucket handle (blue) and pump handle (red) rotations in the four phylogenetically disparate squamate species compared (see interactive plot). Note the opposite pump handle rotation polarity that cluster *Iguana iguana* with *Salvator merianae* and *Boa constrictor* with *Varanus exanthematicus*. (B) Orthogonal view of the relative proportion of bucket handle (blue) and caliper (green) rotations (see Fig. S7). Note the consistent use of predominantly bucket handle rotations for all species and the small caliper contribution to all rib motions except those from one *I. iguana* (Table S1).

rotation magnitude ($F_{1,395.23}$=18.51; P<0.001). Our ANOVA comparison of these two discrete models further confirmed that rib type was one of the strongest predictors of variation in our data (P<0.001), alongside species.

We then used the same multivariate mixed effects models to compare the data of only boas and monitor lizards. We found that comparisons between these two species, accounting for the random effects of individuals, were not significantly different (P=0.92). When we compared species and accounted for random individual effects and the fixed effect of rib type, however, we found that species was similarly not significant (species: P=0.34), while comparisons of rib type were significant (type: P<0.001). The ANOVA comparison of these models also found that inclusion of species and rib type was the strongest predictor of variation in our data (P<0.001).

DISCUSSION

Mechanics of lung ventilation in boa constrictors

Our data indicate that boa constrictors actively modulate their lung ventilation in response to hindered rib motion. Rib motions in vascular and saccular regions were the result of spatially discrete rotations and muscle activation patterns, rather than the byproduct of indiscriminate muscle activation throughout the length of the lung. In almost all X-ray videos, we observed no rib motions (i) under or around the blood pressure cuff or (ii) in unmarked body segments, including those between our marked regions (Fig. 3; Movies 2 and 3). We were also unable to elicit rib motions in the saccular region except when the vascular region was hindered or when the snake hissed, suggesting active recruitment of individual segments in response to these stimuli.

These XROMM findings are further supported by additional EMG and videography data. EMG and video recordings during defensive hissing demonstrate that boas can simultaneously rotate their ribs and activate the LC throughout the length of their trunk. By contrast, EMG signals recorded during defensive posturing are consistent with our XROMM recorded spatially and temporally distinct rib rotations and present further evidence for active recruitment or quiescence of LC activity in response to situational stimuli (Fig. S2). Spatially isolated recruitment of the LC is also not entirely unexpected, as the LC of some elapids is used to move the ribs for defensive hooding and lung ventilation, behaviors that are not mutually exclusive and can occur in tandem or isolation either in the cervical region (hooding) or throughout the trunk (ventilation) (Young and Kardong, 2010). When viewed together, our findings of (i) spatially discrete rib motions in either vascular or saccular regions, (ii) a lack of indiscriminate rib motions throughout the trunk during ventilation, and (iii) regional fluctuations in LC activity or quiescence in disparate segments strongly support our hypothesis. We therefore conclude that boa constrictors can actively modulate the location of lung ventilation throughout their rib cage, a mechanism we refer to as modular lung ventilation.

Moreover, the isolated rib motions demonstrated in this study indicate that respiratory centers within the central nervous system selectively activate musculature around specific ribs, suggesting a neural feedback control not previously described in snakes. As in most amniotes, rib-powered lung ventilation in snakes relies on a complex nervous feedback-control system to match ventilation to metabolic demands, although snakes appear to have weaker vagally mediated reflex responses than other amniotes (Bartlett et al., 1986). Such control systems in snakes include peripheral and central chemoreceptors and mechanoreceptors, cranial nerve afferents, hindbrain inspiratory and expiratory respiratory pattern generators (RPGs), and descending efferent innervation to skeletal muscles that, in turn, drive ventilation (Milsom et al., 2022; Taylor et al., 2010). Given the afferent feedback required to produce the discrete rib coordination in this study, there are several potential neural reflex pathways that could account for the modular ventilation mechanics observed. In one possible scenario, mechano-sensory afferent signals generated from tissues in regions where normal ventilation is compromised may ascend the spinal cord, and directly influence hindbrain RPGs. This could subsequently alter normal descending respiratory motor traffic to the LC and ventilatory musculature in that segment, while simultaneously activating normal respiratory skeletal muscle function in uninvolved regions on either side of the ribs in conflict. An alternative to this sequence could be the short-circuiting of the hindbrain RPGs by local or segmental inhibition of descending respiratory pathways, only at spinal regions where ventilation is compromised. Experimental support for either potential pathway is required and warrants further investigation. Furthermore, additional study of the sensory reception that initiates control is also necessary as a variety of mechano-sensory receptors are potential contributors. These include cutaneous pressure receptors, hypaxial and epaxial skeletal muscle spindles and Golgi tendon mechanoreceptors, and perhaps even intraspinal stretch receptors. While most of these are relatively well characterized, intraspinal stretch receptors are not. Spinal mechanoreceptors play an important role in the coordination of lamprey undulatory locomotion and general proprioception (Grillner et al., 1984; Hsu et al., 2013) and these same receptors have been described in crotaline snakes (Schroeder, 1986). While we cannot directly link their role in the management of modular body cavity expansion and compression during ventilation, their ipsilateral and contralateral segmental connectivity to local and regional motor outflow makes them tantalizing prospects for future research.

Mechanics of rib rotation in squamates

Our comparisons of rib kinematics among squamates indicate that floating ribs have an identifiable kinematic pattern and provide insight into the muscular mechanics of modular ventilation in snakes. When we compared boas with monitors in isolation, we found that the rib rotations of boas were not different from the combined rotations of monitors, yet when we accounted for rib type, we found that floating ribs of boas and monitors were indistinguishable from each other and differed from the vertebral ribs of monitors. It is possible that the lack of sternal ribs in monitors and boas, presumed to be important drivers of inhalation in most amniotes, produces these differences (Brainerd, 2015; De Troyer et al., 2005). However, the vertebral ribs of monitors were more like the floating ribs of boas than the vertebral ribs of iguanas and tegus, suggesting that something other than the lack of sternal connections is responsible for these differences.

The most compelling distinction in our comparison was the polarity of the pump handle rotations. Compared with iguanas and tegus, boas and monitors used larger proportions of pump handle rotations, and these rotations were consistently in the opposite direction from those in iguanas and tegus, potentially as a result of species-specific variation in costal musculature. Most squamates, including iguanas and tegus, rely on intercostal muscles to generate rib rotations during lung ventilation (Brainerd, 2015). Snakes, however, also use the robust LC during inhalation, muscles with caudally oriented ventrolateral lines of action between the vertebrae and ribs (Fig. 1). Contraction along the line of action of the LC would produce the observed cranial pump rotations, particularly

when compared with the intercostals. The LC muscle is found in all snakes, including basal scolecophidians (Gasc, 1981). Moreover, similarly arranged muscles have also recently been described in monitor lizards, including a small LC oriented as in snakes and a large supracostalis brevis, which runs caudally and ventrolaterally from the epaxial aponeuroses to each rib (Cieri, 2018). The presence of the LC and cranial pump handle rotations of the floating ribs in both boas and monitor lizards is evidence that the LC muscles, rather than their lack of ventral articulations, are responsible for the distinctive kinematics of the floating ribs.

Together, these results suggest that the LC muscle is an essential innovation enabling modular lung ventilation mechanics, at least in snakes. Intercostal muscles are not good candidates for producing modular ventilation because they run from rib to rib, linking the ribcage together into an integrated structure. While this linkage does not preclude the intercostals from participating in modular ventilation, this configuration makes intercostals less able to produce the highly regionalized and controlled rib motions observed. Rather, local contraction of intercostals attached to precluded ribs would be damped by the immobility of the ribs and the potential of intercostals on either side of the contraction. In contrast, the LC muscles attach to each rib independently (Fig. 1) and thus are able to actuate each rib separately for modular ventilation. Within squamates, LC are only found in two other taxa, the fossorial amphisbaenians and dibamids, which are also limbless squamates (Gasc, 1981; Leal and Cohn, 2018). Additional research is necessary to understand whether there is a functional relationship between modular lung ventilation, elongation, and limblessness in squamates, including the role of the LC. Such work would reveal whether modular ventilation is only found in snakes and help uncover the historical context and contingencies that produced the high degree of rib control observed in snakes, particularly relative to that in other limbless lizards.

Modular lung ventilation as an innovation of snakes

We propose that modular lung ventilation may have been a necessary innovation during snake evolution before constriction and ingestion of extremely large prey could evolve. Localized lung ventilation has been anecdotally observed in numerous, phylogenetically diverse snake species (e.g. boids, pythonids and colubrids), dating back more than 50 years (Canjani et al., 2003; Greene, 1997; Lillywhite, 2014; McDonald, 1959; Rosenberg, 1973; Wallach, 1998). We present similar observations of such behavior in boas during both constriction and prey ingestion. Moreover, the primary driver of inhalation in snakes, the LC, is found in all snake species, including basal scolecophidians (Gasc, 1981). This suggests that modular ventilation is possibly an ancestral trait for macrostomatan snakes, if not crown Serpentes (Hsiang et al., 2015).

We further suggest that neither constriction nor ingestion of enormous prey could have evolved in the absence of modular lung ventilation because of the high metabolic costs of these behaviors and their interference with normal lung ventilation. Before the evolution of constriction, snakes are thought to have consumed relatively large prey compared with their ancestral squamates, yet still smaller than the prey consumed by extant macrostomatans (Hsiang et al., 2015). Although the evolution of constriction would have enabled early snakes to subjugate heavier (albeit narrow) prey items, this behavior may have incurred substantial metabolic costs (Greene, 1983; Greene, 1997). Extant macrostomatan snakes consume up to 6.8 times more oxygen during constriction relative to resting rates, with a typical event lasting 8–16 min and some extending up to 45 min (Boback et al., 2012; Canjani et al., 2003; Mehta and Burghardt, 2008). The digestion of large prey is similarly expensive, with snakes increasing oxygen consumption between 3- and 17-fold to digest prey roughly 25% of their own mass (Andrade et al., 2004; Greene, 1983; 1997; Overgaard et al., 1999; Secor, 2008; Secor and Diamond, 1998; Toledo et al., 2003). Hence, although snakes maintain a tremendous capacity for anaerobic metabolism, prey subjugation and digestion are among the most aerobic behaviors snakes sustain. These increased rates of oxygen consumption inherently require consistent convection to maintain, as snakes will increase minute ventilation rates 2.5-fold to digest prey only 25% of their own mass (Secor et al., 2000).

These aerobically demanding behaviors may have therefore been difficult to sustain and evolve because of their mechanical interference with lung ventilation. All prey subjugation modes, including complex constriction coils or variable body pinning techniques, engage the cranial one- to two-thirds of the snake's body, a pattern that is consistent throughout the multiple acquisitions of constriction within the clade (Bealor and Saviola, 2007; Boback et al., 2015; Greene and Burghardt, 1978; Mehta and Burghardt, 2008; Moon, 2000). Moreover, this mode of prey subjugation uses the rib cage of the snake to pressurize the rib cage of the prey, with less variable and higher mass-specific forces correlated with more consistent, uniform coil postures, that are presumably more efficient and safer for the snake (Boback et al., 2015; Moon et al., 2019). The LC has also been suggested to be an integral contributor to such behaviors in constricting colubrids, as a result of its control over the ribs in contact with the prey and large physiological cross-sectional area (PCSA), nearly or more than double the PCSA of the other epaxial muscles typically associated with constriction force production (Capano, 2020; Moon, 2000; Penning, 2018). Hence, a conflict may have been present in ancestral snakes, even during less complex body pinning, because of the intrinsic use of the ribs during subjugation and likely involvement of the LC, though more quantitative analyses are needed to understand the mechanics of constriction.

In combination with the findings of this study, this physiological, anatomical and historical evidence indicates a functional relationship between modular lung ventilation, constriction and large prey ingestion. We suggest that neither constriction, including all variable body pinning techniques, nor large prey ingestion could have arisen without some ability to sustain the metabolic costs and intrinsic convection requirements each incurred. Modular lung ventilation could have co-evolved alongside constriction and large prey ingestion, enabling early snakes to accommodate increased metabolic costs and regulate ventilation, as well as co-opt a greater proportion of their trunk to participate in other behaviors, depending on the circumstances. Such discrete spatial shifting of lung ventilation would also have reduced energetic expenditure relative to plausible indiscriminate full lung ventilation, as the latter would either waste energy on actuation of immovable ribs or over-ventilate the lung during periods of inactivity. We therefore infer that early snake species may have been in possession of and employed modular lung ventilation during or prior to the evolution of constriction and large prey ingestion. Without such a mechanism, early snakes would have been unable to circumvent the mechanical and physiological constraints each behavior subsequently produced. This interplay of traits would have enabled early snakes to subdue and ingest a wider variety of prey species and expand their ecological roles beyond those of other elongate vertebrates, facilitating the remarkable radiation of snakes we observe today.

Acknowledgements
The authors thank Erika Tavares for administrative and technical assistance, and Nathan Kley, Stephen Gatesy, Anthony Pires and Thomas Roberts for their expertise and advice. We also thank members of the Brown University Morphology Group for their instrumental surgical and animal husbandry assistance, including Christopher Anderson, Mariana DeBare, Terry Dial, David Boerma, Carolyn Eng, Yordano Jimenez, Elska Kaczmarek, J.D. Laurence-Chasen, Jeremy Lomax, Jillian Oliver, Aaron Olsen, Armita Manafzadeh, Adam Moreno, Sabine Moritz, Miranda Norlin, Andrea Rummel, David Sleboda, Kris Stover, Diego Sustaita, Henry Tsai, Morgan Turner and Hannah Weller. We are immensely grateful for the help of the Brown University Animal Care Facility staff, and, in particular, Seth Hovey and Lara Helwig for their ongoing support throughout the project. We also thank Emment Blankenship for his surgical expertise as well as Jamie Alter, Justin Kiehne, Kyle Ngo and Chris Theodorou for their assistance with experiments and videography at Dickinson College. In addition, we would like to thank Matthew Fuxjager, Daniel Tobiansky, Nigel Anderson, Ghislaine Cardenas-Posada, Nicole Moody, Amy Rutter, Jake Socha and Tobias Wang for their helpful comments on the manuscript.

Competing interests
The authors declare no competing or financial interests.

Author contributions
Conceptualization: J.G.C., S.B., C.Z., E.B.; Methodology: J.G.C., S.B., C.Z., E.B.; Software: J.G.C., H.W.; Formal analysis: J.G.C., H.W.; Resources: S.B., R.C.; Data curation: J.G.C., R.C.; Writing - original draft: J.G.C.; Writing - review & editing: J.G.C., S.B., H.W., R.C., C.Z., E.B.; Visualization: J.G.C.; Supervision: S.B., C.Z., E.B.; Project administration: E.B.; Funding acquisition: J.G.C., E.B.

Funding
This research was partially supported by grant awards to J.G.C. from the Society of Integrative and Comparative Biology Grants-in-Aid of Research program, the Sigma Xi Grants in Aid of Research program [grant numbers G201603152024996 and G2017100190748016], an EEB Dissertation Development Grant from the Drollinger Family Charitable Foundation, the American Society of Ichthyologists and Herpetologist Gaige Fund Award, and the Bushnell Research and Education Fund. This work was also partially supported by grant awards to E.L.B. from the US National Science Foundation [grant numbers 1655756 and 1661129].

Data availability
The raw data used in this study (X-ray video data and CT scan data) are available on the X-ray Motion Analysis Portal (www.xmaportal.org) under permanent ID Brown63: https://xmaportal.org/webportal/larequest.php?request=CollectionView&StudyID=63&instit=BROWN&collectionID=6.

References

Andrade, D. V., De Toledo, L. F., Abe, A. S. and Wang, T. (2004). Ventilatory compensation of the alkaline tide during digestion in the snake *Boa constrictor*. *J. Exp. Biol.* **207**, 1379-1385. doi:10.1242/jeb.00896
Bartlett, D., Mortola, J. P. and Doll, E. J. (1986). Respiratory mechanics and control of the ventilatory cycle in the garter snake. *Respir. Physiol.* **64**, 13-27. doi:10.1016/0034-5687(86)90057-5
Bates, D., Mächler, M., Bolker, B. M. and Walker, S. C. (2015). Fitting linear mixed-effects models using lme4. *J. Stat. Softw.* **67**, 1-48. doi:10.18637/jss.v067.i01
Bealor, M. T. and Saviola, A. J. (2007). Behavioural complexity and prey-handling ability in snakes: Gauging the benefits of constriction. *Behaviour* **144**, 907-929. doi:10.1163/156853907781492690
Bergmann, P. J., Mann, S. D. W., Morinaga, G., Freitas, E. S. and Siler, C. D. (2020). Convergent evolution of elongate forms in craniates and of locomotion in elongate squamate reptiles. *Integr. Comp. Biol.* **60**, 190-201. doi:10.1093/icb/icaa015
Boback, S. M., Hall, A. E., McCann, K. J., Hayes, A. W., Forrester, J. S. and Zwemer, C. F. (2012). Snake modulates constriction in response to prey's heartbeat. *Biol. Lett.* **8**, 473-476. doi:10.1098/rsbl.2011.1105
Boback, S. M., McCann, K. J., Wood, K. A., McNeal, P. M., Blankenship, E. L. and Zwemer, C. F. (2015). Snake constriction rapidly induces circulatory arrest in rats. *J. Exp. Biol.* **218**, 2279-2288. doi:10.1242/jeb.121384
Brainerd, E. L. (2015). Major transformations in vertebrate breathing mechanisms. In *Great Transformations in Vertebrate Evolution* (ed. K. P. Dial, N. Shubin and E. L. Brainerd), pp. 47-62. Chicago: Chicago University Press.
Brainerd, E. L. and Owerkowicz, T. (2006). Functional morphology and evolution of aspiration breathing in tetrapods. *Respir. Physiol. Neurobiol.* **154**, 73-88. doi:10.1016/j.resp.2006.06.003
Brainerd, E. L., Baier, D. B., Gatesy, S. M., Hedrick, T. L., Metzger, K. A., Gilbert, S. L. and Crisco, J. J. (2010). X-ray reconstruction of moving morphology (XROMM): precision, accuracy and applications in comparative biomechanics research. *J. Exp. Zool. Part A Ecol. Genet. Physiol.* **313**, 262-279, doi:10.1002/jez.589
Brainerd, E. L., Moritz, S. and Ritter, D. A. (2016). XROMM analysis of rib kinematics during lung ventilation in the green iguana, *Iguana iguana*. *J. Exp. Biol.* **219**, 404-411, doi:10.1242/jeb.127928
Brandley, M. C., Huelsenbeck, J. P. and Wiens, J. J. (2008). Rates and patterns in the evolution of snake-like body form in squamate reptiles: Evidence for repeated re-evolution of lost digits and long-term persistence of intermediate body forms. *Evolution* **62**, 2042-2064. doi:10.1111/j.1558-5646.2008.00430.x
Brocklehurst, R. J., Moritz, S., Codd, J., Sellers, W. I. and Brainerd, E. L. (2017). Rib kinematics during lung ventilation in the American alligator (Alligator mississippiensis): an XROMM analysis. *J. Exp. Biol.* **220**, 3181-3190. doi:10.1242/jeb.156166
Brocklehurst, R. J., Moritz, S., Codd, J., Sellers, W. I. and Brainerd, E. L. (2019). XROMM kinematics of ventilation in wild turkeys (*Meleagris gallopavo*). *J. Exp. Biol.* **222**, jeb209783, doi:10.1242/jeb.209783
Caldwell, M. W. (2019). *The Origin of Snakes*. Boca Raton: Taylor & Francis, CRC Press.
Canjani, C., Andrade, D. V., Cruz-Neto, A. P. and Abe, A. S. (2003). Aerobic metabolism during predation by a boid snake. *Comp. Biochem. Physiol. Part A* **133**, 487-498. doi:10.1016/S1095-6433(02)00150-2
Capano, J. G. (2020). Reaction forces and rib function during locomotion in snakes. *Integr. Comp. Biol.* **60**, 215-231. doi:10.1093/icb/icaa033
Capano, J. G., Moritz, S., Cieri, R. L., Reveret, L. and Brainerd, E. L. (2019a). Rib motions don't completely hinge on joint design: costal joint anatomy and ventilatory kinematics in a Teiid Lizard, *Salvator merianae*. *Integr. Org. Biol.* **1**, 1-17, doi:10.1093/iob/oby004
Capano, J. G., Cieri, R. L., Weller, H. I. and Brainerd, E. L. (2019b). Ribs All the Way Down: 3D-Rib Kinematics during Lung Ventilation in *Boa constrictor* (Reptilia: Serpentes), Comparison with Three Non-Serpentine Squamates, and Implications for Evolutionary Convergence. *J. Morphol.* 280, pp. S94-S95 doi:10.1002/jmor.21003
Carrier, D. (1989). Ventilatory action of the hypaxial muscles of the lizard *Iguana iguana*: a function of slow muscle. *J. Exp. Biol.* **143**, 435-457. doi:10.1242/jeb.143.1.435
Cieri, R. L. (2018). The axial anatomy of monitor lizards (Varanidae). *J. Anat.* **233**, 636-643. doi:10.1111/joa.12872
Cieri, R. L., Moritz, S., Capano, J. G. and Brainerd, E. L. (2018). Breathing with floating ribs: XROMM analysis of lung ventilation in savannah monitor lizards. *J. Exp. Biol.* **221**, jeb189449, doi:10.1242/jeb.189449
Cohn, M. J. and Tickle, C. (1999). Developmental basis of limblessness and axial patterning in snakes. *Nature* **399**, 474-479. doi:10.1038/20944
De Troyer, A., Kirkwood, P. A. and Wilson, T. A. (2005). Respiratory action of the intercostal muscles. *Physiol. Rev.* **85**, 717-756. doi:10.1152/physrev.00007.2004
Duncker, H.-R. (1978). General Morphological Principles of Amniotic Lungs. In *Respiratory Function in Birds, Adult and Embryonic* (ed. J. Piiper), pp. 2-15. Springer.
Gans, C. (1961). The feeding mechanism of snakes and its possible evolution. *Integr. Comp. Biol.* **1**, 217-227, doi:10.1093/icb/1.2.217
Gans, C. and Maderson, P. F. A. (1973). Sound producing mechanisms in recent reptiles: Review and comment. *Integr. Comp. Biol.* **13**, 1195-1203, doi:10.1093/icb/13.4.1195
Gasc, J.-P. (1981). Axial musculature. In *Biology of the Reptilia* (ed. C. Gans and T. S. Parsons), pp. 355-435. New York: Academic Press.
Gatesy, S. M., Baier, D. B., Jenkins, F. A. and Dial, K. P. (2010). Scientific rotoscoping: a morphology-based method of 3-D motion analysis and visualization. *J. Exp. Zool. A. Ecol. Genet. Physiol.* **313**, 244-261, doi:10.1002/jez.588
Grant, M. M., Brain, J. D. and Vinegar, A. (1981). Pulmonary defense mechanisms in *Boa constrictor*. *J. Appl. Physiol.* **50**, 979-983. doi:10.1152/jappl.1981.50.5.979
Gratz, R. K., Amos, A. R. and Geiser, J. (1981). Gas tension profile of the lung of the viper, *Vipera xanthina palestinae*. *Respir. Physiol.* **44**, 165-176. doi:10.1016/0034-5687(81)90035-9
Greene, H. W. (1983). Dietary correlates of the origin and radiation of snakes. *Am. Zool.* **23**, 431-441. doi:10.1093/icb/23.2.431
Greene, H. W. (1997). *Snakes: The Evolution of Mystery in Nature*. Berkley: University of California Press.
Greene, H. W. and Burghardt, G. M. (1978). Behavior and phylogeny: constriction in ancient and modern snakes. *Science* **200**, 74-77. doi:10.1126/science.635575
Grillner, S., Williams, T. and Lagerbäck, P. Å. (1984). The edge cell, a possible intraspinal mechanoreceptor. *Science* **223**, 500-503. doi:10.1126/science.6691161
Grood, E. S. and Suntay, W. J. (1983). A joint coordinate system for the clinical description of three-dimensional motions: application to the knee. *J. Biomech. Eng.* **105**, 136-144. doi:10.1115/1.3138397
Guerrero, J. A. and Macías-Díaz, J. E. (2014). A computational method for the detection of activation/deactivation patterns in biological signals with three levels of electric intensity. *Math. Biosci.* **248**, 117-127. doi:10.1016/j.mbs.2013.12.010

Head, J. J. and Polly, P. D. (2015). Evolution of the snake body form reveals homoplasy in amniote Hox gene function. *Nature* **520**, 86-89. doi:10.1038/nature14042

Hoffstetter, R. and Gasc, J.-P. (1969). Vertebrae and Ribs of Modern Reptiles. In *Biology of the Reptilia*, vol. 1, pp. 319-337. Oxford University Press.

Hsiang, A. Y., Field, D. J., Webster, T. H., Behlke, A. D., Davis, M. B., Racicot, R. A. and Gauthier, J. A. (2015). The origin of snakes: revealing the ecology, behavior, and evolutionary history of early snakes using genomics, phenomics, and the fossil record. *BMC Evol. Biol.* **15**, 87, doi:10.1186/s12862-015-0358-5

Hsu, L.-J., Zelenin, P. V., Grillner, S., Orlovsky, G. N. and Deliagina, T. G. (2013). Intraspinal stretch receptor neurons mediate different motor responses along the body in lamprey. *J. Comp. Neurol.* **521**, 3847-3862. doi:10.1002/cne.23382

Kardong, K. V. (1972). Morphology of the respiratory system and its musculature in different snake genera. Part II. *Charina bottae*. *Gegenbaurs Morphol. Jahrb.* **117**, 364-376.

Knörlein, B. J., Baier, D. B., Gatesy, S. M., Laurence-Chasen, J. D. and Brainerd, E. L. (2016). Validation of XMALab software for marker-based XROMM. *J. Exp. Biol.* **219**, 3701-3711, doi:10.1242/jeb.145383

Kuznetsova, A., Brockhoff, P. B. and Christensen, R. H. B. (2017). lmerTest package: tests in linear mixed effects models. *J. Stat. Softw.* **82**, 1-26. doi:10.18637/jss.v082.i13

Landberg, T., Mailhot, J. D. and Brainerd, E. L. (2003). Lung ventilation during treadmill locomotion in a terrestrial turtle, *Terrapene carolina*. *J. Exp. Biol.* **206**, 3391-3404. doi:10.1242/jeb.00553

Leal, F. and Cohn, M. J. (2018). Developmental, genetic, and genomic insights into the evolutionary loss of limbs in snakes. *Genesis*, **56**, e23077, doi:10.1002/dvg.23077

Lillywhite, H. B. (2014). *How Snakes Work*. Oxford, UK: Oxford University Press.

Longrich, N. R., Bhullar, B.-A. S. and Gauthier, J. A. (2012). A transitional snake from the Late Cretaceous period of North America. *Nature* **488**, 205-208. doi:10.1038/nature11227

McDonald, H. S. (1959). Respiratory functions of the Ophidian Air Sac. *Herpetologica* **15**, 193-198.

Mehta, R. S. and Burghardt, G. M. (2008). Contextual flexibility: Reassessing the effects of prey size and status on prey restraint behaviour of macrostomate snakes. *Ethology.* **114**, 133-145. doi:10.1111/j.1439-0310.2007.01437.x

Menegaz, R. A., Baier, D. B., Metzger, K. A., Herring, S. W. and Brainerd, E. L. (2015). XROMM analysis of tooth occlusion and temporomandibular joint kinematics during feeding in juvenile miniature pigs. *J. Exp. Biol.* **218**: 2573-2584. doi:10.1242/jeb.119438

Milsom, W. K., Kinkead, R., Hedrick, M. S., Gilmour, K., Perry, S., Gargaglioni, L. and Wang, T. (2022). Evolution of vertebrate respiratory central rhythm generators. *Respir. Physiol. Neurobiol.* **295**, 103781. doi:10.1016/j.resp.2021.103781

Moon, B. R. (2000). The mechanics and muscular control of constriction in gopher snakes (*Pituophis melanoleucus*) and a king snake (*Lampropeltis getula*). *J. Zool.* **252**, 83-98. doi:10.1111/j.1469-7998.2000.tb00823.x

Moon, B. R., Penning, D. A., Segall, M. and Herrel, A. (2019). *Feeding in snakes: form, function, and evolution of the feeding system*. In *Feeding in vertebrates: evolution, morphology, behavior, biomechanics* (ed. V. Bels and I. Q. Whisaw), pp. 528-574. Switzerland: Springer Nature.

Osmond, D. G. (1985). Functional anatomy of the chest wall. In *The Thorax* (ed. C. Roussos and P. T. Macklem), pp. 199-233. New York: Marcel Dekker, Inc.

Overgaard, J., Busk, M., Hicks, J. W., Jensen, F. B. and Wang, T. (1999). Respiratory consequences of feeding in the snake *Python molorus*. *Comp. Biochem. Physiol. - A Mol. Integr. Physiol.* **124**, 359-365. doi:10.1016/S1095-6433(99)00127-0

Penning, D. A. (2018). Quantitative axial myology in two constricting snakes: *Lampropeltis holbrooki* and *Pantherophis obsoletus*. *J. Anat.* **232**, 1016-1024. doi:10.1111/joa.12799

Rosenberg, H. I. (1973). Functional anatomy of pulmonary ventilation in the garter snake, Thamnophis elegans. *J. Morphol.* **140**, 171-184. doi:10.1002/jmor.1051400205

Schroeder, D. M. (2009). An ultrastructural study of the marginal nucleus, the intrinsic mechanoreceptor of the Snake's spinal cord. *Somatosens. Res.* **4**, 127-140. doi:10.3109/07367228609144602

Secor, S. M. (2008). Digestive physiology of the Burmese python: broad regulation of integrated performance. *J. Exp. Biol.* **211**, 3767-3774, doi:10.1242/jeb.023754

Secor, S. M. and Diamond, J. (1998). A vertebrate model of extreme physiological regulation. *Nature* **395**, 659-662. doi:10.1038/27131

Secor, S. M., Hicks, J. W. and Bennett, A. F. (2000). Ventilatory and cardiovascular responses of a python (Python molurus) to exercise and digestion. *J. Exp. Biol.* **203**, 2447-2454. doi:10.1242/jeb.203.16.2447

Taylor, E. W., Leite, C. A. C., McKenzie, D. J. and Wang, T. (2010). Control of respiration in fish, amphibians and reptiles. *Brazilian J. Med. Biol. Res.* **43**, 409-424. doi:10.1590/S0100-879X2010007500025

Toledo, L. F., Abe, A. S. and Andrade, D. V. (2003). Temperature and meal size effects on the postprandial metabolism and energetics in a boid snake. *Physiol. Biochem. Zool.* **76**, 240-246. doi:10.1086/374300

Uetz, P., Cherikh, S., Shea, G., Ineich, I., Campbell, P. D., Doronin, I. V., Rosado, J., Wynn, A., Tighe, K. A., McDiarmid, R. et al. (2019). A global catalog of primary reptile type specimens. *Zootaxa* **4695**, 438-450. doi:10.11646/zootaxa.4695.5.2

Wallach, V. (1998). The lungs of snakes. In *Biology of the Reptilia: Morphology G.* vol. 19 (ed. C. Gans), pp. 93-295. Ithaca, NY: Society for the Study of Amphibians and Reptiles.

Wiens, J. J., Brandley, M. C., Reeder, T. O. D. W. (2006). Why Does a Trait Evolve Multiple Times within a Clade? Repeated Evolution of Snakelike Body Form in Squamate. *Evolution* **60**, 123-141.

Young, B. A. and Kardong, K. V. (2010). The functional morphology of hooding in cobras. *J. Exp. Biol.* **213**, 1521-1528. doi:10.1242/jeb.034447